

Energy and Nvidia Sionna-Based Signal Integrity: Selection Design for Off-the-Shelf Synthetic Aperture Radar-Capable Unmanned Aerial Vehicles

Victor B. Calinao Jr.^{1*}, Edwin Sybingco¹, Argel A. Bandala¹, and Lawrence Materum^{1,2}

¹Department of Electronics and Computer Engineering, Gokongwei College of Engineering, De La Salle University, Philippines

²Tokyo City University, Japan

*Email: victor_calinaojr@dlsu.edu.ph

Abstract—This paper presents the relationship between energy and signal integrity of Unmanned Aerial Vehicles (UAVs) with Synthetic Aperture Radar (SAR) capabilities for a more informed off-the-shelf selection design. The energy is expressed in the UAV and SAR power consumption, whereas signal integrity is expressed in Bit-Error Rate (BER). Low-end, mid-end, and high-end—categorized in terms of their market cost—commercial UAVs and SAR modules were considered. The energy relations are based on the UAV flight path and power ratings. The signal processing and decomposition of the reconstructed objects for the model simulations are based on a transmit-channel-receive chain of 16-quadrature-amplitude, low-density parity check, Rayleigh response, and single-antenna directivity done through Nvidia Sionna. The results indicate that far-reaching flight spatial path scanning is achieved with high-end UAVs and low-cost SARs, but the accuracy is relatively low. Higher accuracy is achieved with low-end UAVs with high-cost SARs. Further, the results point out that selecting UAV-SAR is critical in terms of energy and accuracy for a specific target application. The outcomes show tradeoffs in the selection design.

Index Terms—Synthetic Aperture Radar (SAR), Unmanned Aerial Vehicles (UAV), Bit-Error Rate (BER), rayleigh fading, nvidia sionna, energy, signal integrity, selection design

I. INTRODUCTION

Synthetic Aperture Radar (SAR) sensors in Unmanned Aerial Vehicles (UAVs) have been gaining popularity and allowed flexible surface observation in different practical applications in medium-scale observation areas such as topographical mapping [1], object detection [2]–[3], and phenotyping [4]. Growing potential use of large and small UAVs for SAR imaging [5]–[7] opens the democratization of SAR. It increases potential applications in scientific, maritime, earth monitoring, and agricultural monitoring.

Early adopters of using UAVs equipped with camera sensors or synthetic apertures in agriculture enjoy the benefit of in-situ data characterization of growing crops

and apply specific interventions that can maximize crop yield and profits [5]. However, the current allowable operation for UAV-equipped SAR sensors can generally be as short as 5 minutes and as long as 55 minutes [8] with factors such as the energy expenditure of the SAR sensor versus its accuracy and the energy capacity of the battery. Providing accurate data characterization is essential but requires more energy. The sweet spot for compensation between energy and signal integrity varies between each UAV and SAR module.

Research in energy and signal integrity relationships in UAVs and SAR modules is not well explored. Simulating signal integrity over a certain channel can be complicated and computationally heavy. It would take a very long time to execute. The authors would like to contribute to this gap and present the relationship between the overall energy expenditure of three UAVs with a SAR sensor and its BER following the simulations based on a transmit-channel-receive chain of 16-quadrature-amplitude (16-QAM), low-density parity-check (LDPC), independent and identically distributed Rayleigh fading channel, and single-antenna directivity done through Nvidia Sionna, an open-source link-layer simulation tool [9] that will ease the execution complexity with reduced simulation time. This work aims to guide future adopters in designing off-the-shelf commercial UAVs and SAR modules. The selection design guidance provided by authors can cut unnecessary costs or circumvention of choosing an excessive specification for a particular UAV or SAR module application in an intended mission. Section II discusses the system design. It is followed by the discussion of the results in Sec. III. Lastly, summative remarks are given in Sec. IV.

II. DESIGN OF THE SYSTEM

A. Signal Fading: BER against E_b/N_0 Analysis under Rayleigh Fading

In the case of SAR that relies on moving azimuth, each point scatterer on the ground has a different Doppler frequency shift which causes the signals to be received to have fading characteristics. These fading signal characteristics are complicated to simulate and

Manuscript received August 15, 2022; revised December 15, 2022; accepted January 2, 2023.

computationally heavy. Recently, Nvidia Sionna, a GPU-accelerated TensorFlow-based library for simulating the physical layer of wireless communication systems, was released.

The authors maximized the tool to test the performance of the SAR in UAV by getting the Bit-Error Rate (BER) against the ratio of bit energy to noise power spectral density (E_b/N_0) under the Rayleigh fading model in Nvidia Sionna [9].

Fig. 1 shows the architectural block diagram of the system model for a simulation of SISO transmissions over a flat-fading channel that approximates real-world wireless transmissions [10]. An instance of flat-fading channel class was created to simulate transmissions over an independent and identically distributed Rayleigh fading channel.

A point-to-point transmission from the transmitter antenna to the SAR's receiver antenna was investigated. The simulation uses no precoding, and each antenna sends its own data stream.

A batch of random transmit vectors of random 16QAM symbols are generated as the binary source. The low-density parity-check (LDPC) code module is used in the system model as a compliant encoder and a corresponding decoder.

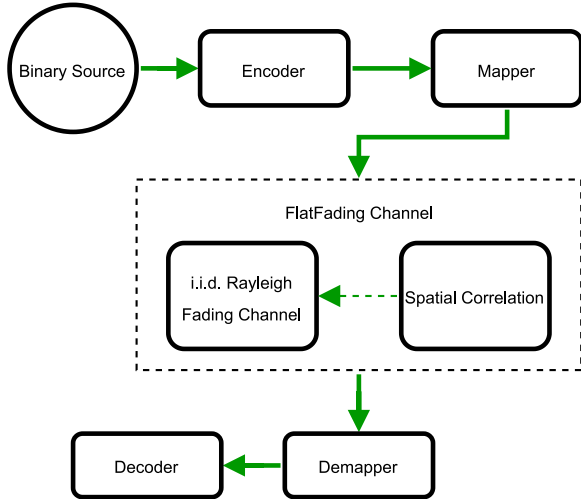


Fig. 1. SISO SAR over flat-fading channel block diagram model

The FlatFading Channel uses the Kronecker correlation model using exponential correlation matrices to add spatial correlation to an independent and identically distributed Rayleigh fading channel.

Computing error rates such as BER are used for characterization and help future system designers choose the best methods for mitigating errors.

The Bit Error Rate (BER) is a critical metric for evaluating systems that transfer digital data from one location to another. Data are prone to errors that are introduced into the system when data is transmitted across a data link. BER measures a system's overall performance, including the transmitter, receiver, and connecting medium.

BER is the error rate of binary signals that occurs in a transmission system and is described in eq. 1.

$$BER = \frac{B_e}{B_s} \quad (1)$$

where B_e , is the total number of bit errors and B_s is the total number of bits sent.

The assumptions of the classical SAR image generation model led to a Rayleigh distribution model [11]. The return signal comprises numerous separate complex signals that fluctuate as the relative magnitudes and phases of the scatterers change geographically. The envelope fluctuation, a linear detector that outputs the magnitude of the envelope voltage, reveals that it follows a Rayleigh distribution. For Rayleigh fading, the ratio of the square of the envelope means to the variance of the fluctuating component is a form of inherent signal-to-noise ratio. The Rayleigh distribution is given by eq. 2.

$$P(r) = \frac{r}{\sigma^2} e^{(-r^2/\sigma^2)}, \quad 0 \leq r \leq \infty \quad (2)$$

where σ is the rms value of the received signal, $r^2/2$ is the instantaneous power, and σ^2 is the local average power of the received signal before detection.

B. UAV and SAR Specifications

In this paper, three UAVs with SAR are selected [7], [12], [13] as the benchmark platform for comparisons that represents low-end, mid-end, and high-end UAVs, respectively. The classifications were based on the cost or the suggested retail price (SRP) of the respective commercial drones at the time of their releases.

The mentioned UAVs with SAR modules are chosen by their availability. Most have been used in personal, educational, commercial, and industrial settings. The extracted specifications in their respective datasheets were the UAV battery energy capacity, UAV power consumption, SAR power consumption, and UAV plus SAR weight. Table I shows the summary of the specifications.

TABLE I: UAV AND SAR SPECIFICATION SUMMARY

UAV / SAR	Battery Energy Capacity	UAV Power Consumption	SAR Power Consumption	UAV plus SAR weight
DJI Phantom 2 / Time Domain PulsON 410	11.1V, 5200mAh, 57.72Wh	130W	4.2 W	1 kg, 58 g
Spreading Wings S900 / INRAS RDL-77G-TX2RX16	22.2V, 12000mAh, 266.4Wh	1000W	11.1W	6.8 kg, 60 g
Matrice 600 Pro / 77 GHz FPGA mmWave	51.2V, 12960mAh, 663.552Wh	1250W	25.6W	10kg, 3kg

The specifications were extracted from the manufacturer's respective datasheets. Some information is not directly extracted from the datasheet, as some are not explicitly.

Because LiPo batteries, such as those used on the selected UAVs, are easily degraded if fully or 100% discharged [14], the authors use a conservative 80% of each UAV's electric charge to compute battery capacity, as shown in Table II.

TABLE II: UAV USEABLE BATTERY CAPACITY ENERGY

UAV	Battery Voltage, (V)	Total Battery Capacity, (mAh)	Useable Battery Capacity, (mAh)
DJI Phantom 2	11.1	5200	4160
Spreading Wings S900	22.2	12000	9600
Matrice 600 Pro	51.2	12960	10368

The power P expressed in watts shown in Table III of an electrical device is equal to the voltage V multiplied by the current I , according to Ohm's law. We multiply both sides of the equation by time to determine the energy stored in a battery since energy is power multiplied by time:

$$E = V \cdot I \cdot T \quad (3)$$

Remember that ampere-hours are a unit of measurement for the electric charge Q in the battery.

$$E = V \cdot Q, \quad (4)$$

where E is the energy stored in a battery, expressed in watt-hours, V is the voltage of the battery, and Q is the electric charge capacity of the battery in amp-hours.

TABLE III: UAV WEIGHT AND POWER CONSUMPTION

UAV	UAV weight, (g)	Total Power Consumption, (W)
DJI Phantom 2	1000	130
Spreading Wings S900	6800	1000
Matrice 600 Pro	10000	1250

In its electrical parameters datasheet [9], INRAS RDL-77G-TX2RX16 specifies three supply currents and voltages, with maximum supply voltages of 3.4 V, 5.1 V, and 3.4 V, and supply currents of 2100 mA, 200 mA, and 860 mA, respectively which computes as its SAR power consumption to be 11.1 W. The other SAR sensor parameters are extracted directly from publicly available data sheets.

TABLE IV. SAR WEIGHT AND POWER CONSUMPTION

SAR	SAR weight, (g)	Total Power Consumption, (W)
Time Domain PulsON 410	58	4.2
INRAS RDL-77G-TX2RX16	60	11.1
77 GHz FPGA mmWave	3000	25.6

The overall power consumption of the SAR and its related weight are shown in Table IV.

The total power consumption of the UAV and SAR can be computed by summing the UAV power consumption and SAR power consumption.

$$f_c = \sum_n^N f_{UAV} + f_{SAR} \quad (5)$$

where f_p is the total power consumption in, f_{UAV} is the power consumption of the UAV, and f_{SAR} is the power consumption of SAR in watts.

TABLE V: UAV SAR ALL UP WEIGHT AND POWER CONSUMPTION

UAV and SAR	All up Weight, (kg)	Total Power Consumption, (W)
DJI Phantom 2	1.058	134.2
Spreading Wings S900	6.860	1011.1
Matrice 600 Pro	10.300	1275.6

C. Flight Path: UAV Grid Flight Path Planning

Drone grid flight paths are ideal for mapping missions, especially in areas where SAR is commonly used to capture data images for processing.

A web-based grid flight planning application [15] was used to set a pre-determined flight path. The drone flight path proprietary algorithm of the mentioned application was used to calculate the time needed to map 32.52 hectares of farmland in Silang, Cavite. Fig. 2 shows the 2D drone grid path plan.



Fig. 2. Drone grid path simulation

The parameters used were 70% side lap and front lap with a cruising altitude of 100 meters. The average speed of the UAV is 20 kilometers per hour. The calculated time to map the target dimensions was 24 minutes.

D. Relationship of Bit Error Rate and Power Consumption for Different Types of UAV

The duration to scan the coverage area t_{COV} is known with our grid path plan and can be converted into an $M \times 1$ matrix, spliced per minute. Hence, we can calculate the energy consumption of the UAV. The energy consumption of the UAV is dependent on the voltage V and power rating Ah .

$$E_{UAV} = Wh = V \cdot Ah \quad (6)$$

Assume that the energy available for SAR E_{SAR} is dependent on the energy capacity of the UAV.

$$E_{SAR} = E_{UAV} = Wh = W[t_{COV}]^T \quad (7)$$

Then we can impose E_{SAR} to be a function of time by multiplying the power consumed by SAR with the vector t_{COV} .

Assume that E_{SAR} uses energy per bit E_b and neglects the energy for the amplifier, impedance matching circuits, band-pass filter, and antenna that usually consume the energy.

Assume that the noise density is constant from all the vectors of the matrix t_{COV} . Since the location is relatively flat, the temperature would be the same. The temperature used in this simulation is 30 degrees centigrade.

$$N_0 = kT = \left(\frac{W}{Hz}\right), \quad (8)$$

Power consumption can now be plotted after the computation. It is assumed that the equation expressed means that the system that requires power is the UAV and the SAR system only.

$$f_c = f_e + f_m = f_{SAR} + f_{UAV} \quad (9)$$

Overall power consumption is f_c , and f_e denotes all electrical power consumption which is from SAR, f_m denotes all the mechanical power consumption which is from the UAV.

Getting the power of SAR in terms of time (t),

$$f_{SAR}(t) = E_{SAR}(t) = E_b(t) \quad (10)$$

where (t), is equal to the matrix t_{COV} expressed in vector form, f_{SAR} and f_{UAV} is expressed in an $M \times 1$ matrix. We then derive Table VI.

TABLE VI: MATRIX TABLE

M	Eb/N0 (dB)	BER (unitless)	f_{SAR} $M \times 1$	f_{UAV} $M \times 1$	f_c $M \times 1$ (Wh)
1	dB		Wh	Wh	Wh
...
M	dB		Wh	Wh	Wh

Generally, the lower the value of the BER, the better the performance. Radars, including SAR, depends on the reflected information or the backscatter. In this paper, the reflected data are affected by the Kronecker with low correlation. The relationship between BER and a UAV's power consumption with SAR sensor operating at the discussed methodology is investigated.

III. RESULTS AND DISCUSSIONS

A. Signal Fading: BER against Eb/N0 Analysis under Rayleigh Fading

E_b/N_0 is the normalized signal-to-noise ratio equal to the SNR divided by the "gross" link spectral efficiency in

(bit/s)/Hz, where the bits in this context are transmitted data bits, including error correction information and other protocol overhead. The computed BER versus the spectral noise density in a SISO SAR over i.i.d Rayleigh channel is shown in Fig. 3. SISO SAR configuration relies on the chirp waveform transmitted signal [16], which is the basic SAR configuration.

Additionally, LDPC encoding and decoding method and Kronecker low correlation model have been treated with the simulation for a low noise performance to meet the reduced transmit power without losing signal-to-noise ratio and thus avoid expensive transmitter [17].

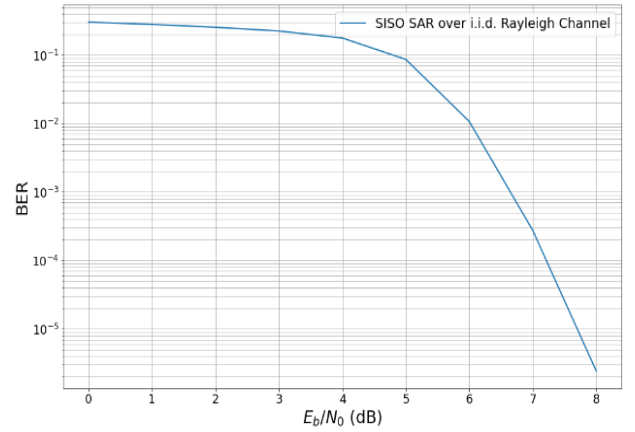


Fig. 3. BER vs. Eb/N0 over i.i.d. Rayleigh fading channel

The Monte-Carlo simulation model shows that it has a good performance with low error rates occurring as low as $E_b/N_0 = 9$ dB.

B. Relationship of BER and Power Consumption for Different UAV SAR

1) Low-end UAV with low-end SAR

The DJI Phantom 2 has a total 4160 mAh useable battery capacity and is considered low-end as the SRP cost suggests compared to the other UAVs in this paper. Fig. 4 shows the scatter plot results with a linear regression coefficient of determination of $R^2 = 0.0235$.

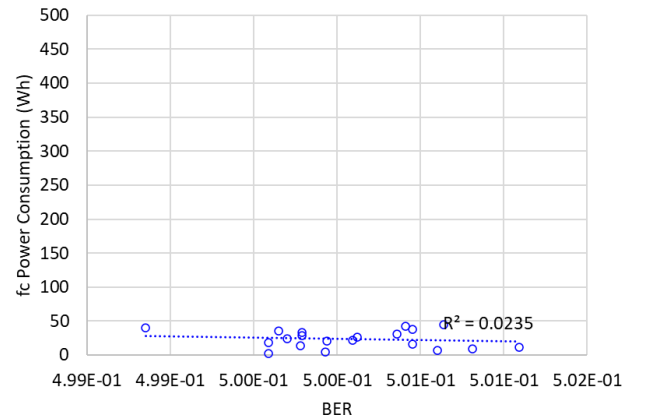


Fig. 4. Power consumption vs. BER of DJI Phantom 2 with SAR

2) Mid-end UAV with mid-end SAR

The Spreading Wings S900 has a total 9600 mAh useable battery and is considered the in-between as the

high-end is the successor of this UAV and costs significantly less. Fig. 5 shows the results with a linear regression coefficient of determination of $R^2 = 0.1017$.

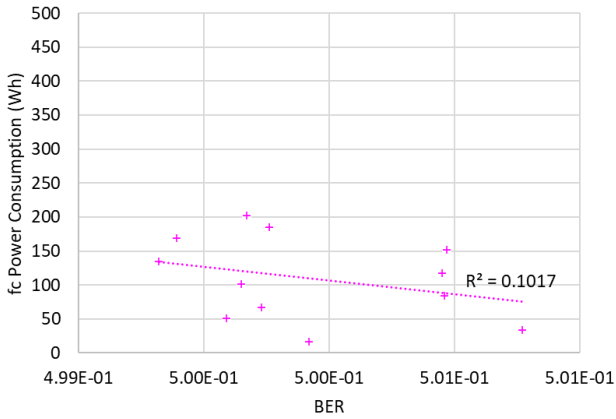


Fig. 5. Power consumption vs. BER of DJI Phantom 2 with SAR

3) *High-end UAV with high-end SAR*

The Matrice 600 Pro has a total 10368 mAh useable battery capacity and is considered high-end as it is the heaviest but has the longest flight time. Fig. 6 shows the results with linear regression of $R^2 = 0.0239$.

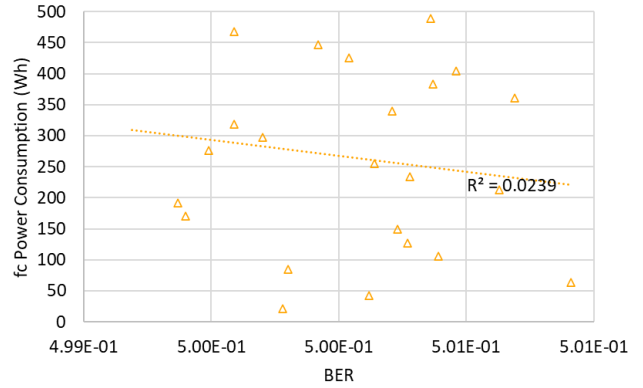


Fig. 6. Power consumption vs. BER of DJI Phantom 2 with SAR

Fig. 7 shows the energy and signal integrity relationships of three UAV and SAR modules with linear regression. It shows that high-end UAVs show a steeper downward slope, which suggests that increasing power consumption leads to lower BER. However, with low-end UAVs, the same BER value could also be obtained with less power consumption. The results also indicate that low-end UAVs show a leveled slope which implies minimal effect on the BER as the energy varies. In the case of mid-end UAVs, it shows performance between high-end and mid-end UAVs.

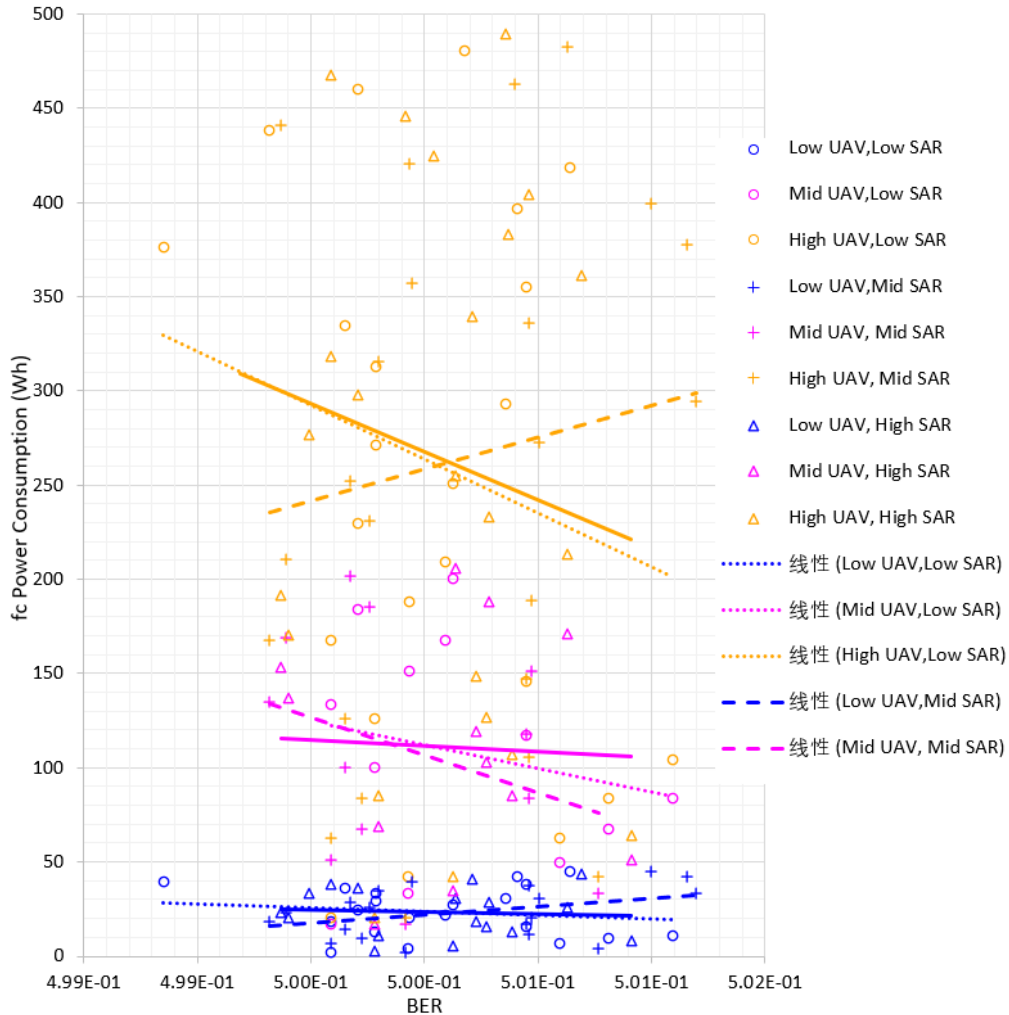


Fig. 7. Power consumption vs. BER of all UAV and SAR combinations

The steepest downward slope of energy and signal integrity UAV and SAR combination is the high-end UAV with low-cost SAR. The most balanced performance is the low-end UAV and high-cost SAR combination.

IV. CONCLUSION

The simulation of commercial UAVs with SAR sensors in a flight grid path determined the relationship between the total power consumption of the system and its accuracy in BER. The model result does not directly describe much of the variance in the dependent variable in the matrices presented as observed in the calculated coefficient of determination R^2 . The Monte-Carlo simulation model from Sionna recorded nominal error rates at $E_b/N_0 = 9.0$ dB and above. Additionally, the coefficient of determination R^2 from the three UAVs follows the same linear regression of downward slope, which indicates that higher power consumption garners lower BER with much intensity on high-end UAVs. The mid-end UAVs follow the downward slope pattern but with much less intensity relatively. The low-end UAV shows the least slope relationship. Generally, the simulation showed a predictable accuracy pattern regarding the system's power consumption.

While low-end, mid-end, and high-end commercial UAVs and SAR modules were considered, the results indicate that far-reaching flight spatial path scanning is achieved with high-end UAVs and low-cost SARs. However, the accuracy is relatively low, and higher accuracy is achieved with low-type UAVs with high-cost SARs. Furthermore, the results point out that selecting UAV-SAR is critical in terms of energy and accuracy for the target application, which shows tradeoffs in the selection design.

CONFLICT OF INTEREST

The authors declare no conflict of interest.

AUTHOR CONTRIBUTIONS

V. B. Calinao Jr. conducted the work, gathered the data, and ran the simulations. E. Sybingco, A. A. Bandala, and L. Materum improved the paper.

ACKNOWLEDGMENT

The authors wish to thank De La Salle University for its support.

REFERENCES

- [1] M. Lort, A. Aguasca, C. López-Martínez, and T. M. Marín, "Initial Evaluation of SAR Capabilities in UAV Multicopter Platforms," *IEEE Journal of Selected Topics in Applied Earth Observations and Remote Sensing*, vol. 11, no. 1, pp. 127–140, Jan. 2018.
- [2] K. Gromada, B. Siemiątkowska, W. Stecz, K. Płochocki, and K. Woźniak, "Real-Time object detection and classification by UAV equipped with SAR," *Sensors (Basel)*, vol. 22, no. 5, p. 2068, Mar. 2022.
- [3] E. Schreiber, A. Heinzl, M. Peichl, M. Engel, and W. Wiesbeck, "Advanced buried object detection by multichannel, UAV/Drone carried synthetic aperture radar," in *Proc. 13th European Conference on Antennas and Propagation (EuCAP)*, Mar. 2019, pp. 1–5.
- [4] G. Yang, *et al.*, "Unmanned aerial vehicle remote sensing for field-based crop phenotyping: Current status and perspectives," *Frontiers in Plant Science*, vol. 8, 2017.
- [5] V. C. Koo, *et al.*, "A new unmanned aerial vehicle synthetic aperture radar for environmental monitoring," *Progress in Electromagnetics Research*, vol. 122, pp. 245–269, Dec. 2011.
- [6] S. I. Tsunoda, *et al.*, *Lynx: A High-Resolution Synthetic Aperture Radar*, vol. 5. 2000, p. 58.
- [7] C. J. Li and H. Ling, "Synthetic aperture radar imaging using a small consumer drone," in *Proc. IEEE International Symposium on Antennas and Propagation USNC/URSI National Radio Science Meeting*, Jul. 2015, pp. 685–686.
- [8] C. W. Chan and T. Y. Kam, "A procedure for power consumption estimation of multi-rotor unmanned aerial vehicle," *J. Phys.: Conf. Ser.*, vol. 1509, no. 1, p. 012015, Apr. 2020.
- [9] J. Hoydis, *et al.*, *Sionna: An Open-Source Library for Next-Generation Physical Layer Research*, 2022.
- [10] Jun Li, A. Bose, and Y. Q. Zhao, "Rayleigh flat fading channels and Capacity," in *Proc. 3rd Annual Communication Networks and Services Research Conference (CNSR'05)*, Halifax, NS, Canada, 2005, pp. 214–217.
- [11] E. Kuruoglu and J. Zerubia, "Modeling SAR images with a generalization of the rayleigh distribution," *Image Processing, IEEE Transactions on*, vol. 13, pp. 527–533, May 2004.
- [12] A. Bekar, M. Antoniou, and C. J. Baker, "Low-Cost, high-resolution, drone-borne SAR imaging," *IEEE Trans. Geosci. Remote Sensing*, vol. 60, pp. 1–11, 2022.
- [13] S. Kim, *et al.*, "Multichannel W-Band SAR system on a multirotor UAV platform with real-time data transmission capabilities," *IEEE Access*, vol. 8, pp. 144413–144431, 2020.
- [14] J. Castro, C. Flores, D. Gonzalez, V. Quintero, and A. Perez, "From the Air to the Ground: An Experimental Approach to Assess LiPo Batteries for a Second Life," in *Proc. Prognostics and Health Management Conference (PHM-2022 London)*, May 2022, pp. 489–494.
- [15] Measure | Ground Control. [Online]. Available: <https://gc.measure.com/login>
- [16] S. Méric and J. Y. Baudais, "Waveform design for MIMO radar and SAR application," in *Topics in Radar Signal Processing*, G. Weinberg, Ed. InTech, 2018.
- [17] H. Essen, W. Johannes, S. Stanko, R. Sommer, A. Wahlen, and J. Wilcke, "High resolution W-band UAV SAR," in *Proc. IEEE International Geoscience and Remote Sensing Symposium*, Jul. 2012, pp. 5033–5036.

Copyright © 2023 by the authors. This is an open access article distributed under the Creative Commons Attribution License ([CC BY-NC-ND 4.0](https://creativecommons.org/licenses/by-nc-nd/4.0/)), which permits use, distribution and reproduction in any medium, provided that the article is properly cited, the use is non-commercial and no modifications or adaptations are made.



Victor B. Calinao Jr. finished his degree on Bachelor of Science in Electronics Engineering in Polytechnic University of the Philippines in 2020 under the scholarship of Commission on Higher Education. A month after graduation he started his employment career as a Systems Design Engineer at Analog Devices, Inc. until he pursued his

degree on Master of Science in Electronics and Communication Engineering as a full time student from De La Salle University, Philippines under the scholarship of Engineering Research and Development for Technology. His research interest generally ranges from remote sensing, IoT, solar energy, and machine learning.



Edwin Sybingeo is a faculty of the De la Salle University ECE Department. He completed his Doctoral of Philosophy in Electronics and Communications Engineering in DLSU area of Digital Signal Processing (DSP) focusing on Big Data and Intelligent Systems. He received his Master of Science

(Electronics and Communications Engineering) from De La Salle University. He already published more than 30 scientific papers internationally in the field of DSP, Machine Vision, Computational Intelligence, and robotics.



Argel A. Bandala received his Bachelor of Science in Electronics and Communications Engineering from Polytechnic University of the Philippines in 2008. He received his Master of Science in Electronics and Communication s Engineering and Doctor of Philosophy in Electronics and Communications

Engineering from De La Salle University in 2012 and 2015 respectively. He is currently a Full Professor and Research Faculty at De La Salle University. His research interests are artificial intelligence, algorithms, software engineering, automation, and swarm robotics. Dr. Bandala is very active in the IEEE Philippine Section where he served as the Section Secretary for the years 2012 to present. He also serves as the secretary of IEEE Computational Intelligence Society Philippine Section from 2012 to present. He is also an active member of the IEEE Robotics and Automation Society from 2013 to present.



Lawrence Materum received the B.Sc. degree in electronics and communications engineering with honors from Mapúa Institute of Technology (now Mapúa University),s the M.Sc. degree in electrical engineering major in computers and communications from the University of the Philippines Diliman through an

Analog Devices Fellowship, and the Ph.D. degree in international development engineering (major in electrical/ electronics engineering) from Tokyo Institute of Technology through a MEXT Scholarship.